JCTC Journal of Chemical Theory and Computation

Modeling Proton Transfer in Zeolites: Convergence Behavior of Embedded and Constrained Cluster Calculations

Justin T. Fermann,[†] Teresa Moniz,[†] Oliver Kiowski,[†] Timothy J. McIntire,[†] Scott M. Auerbach,*[,†,‡] Thom Vreven,[§] and Michael J. Frisch[§]

Departments of Chemistry and Chemical Engineering, University of Massachusetts, Amherst, Massachusetts 01003, and Gaussian, Inc., 340 Quinnipiac Street, Building 40, Wallingford, Connecticut 06492

Received May 2, 2005

Abstract: We have studied the convergence properties of embedded and constrained cluster models of proton transfer in zeolites. We applied density functional theory to describe clusters and ONIOM to perform the embedding. We focused on converging the reaction energy and barrier of the O(1) to O(4) jump in H−Y zeolite as well as vibrational and structural aspects of this jump. We found that using successively larger clusters in vacuo gives convergence of this reaction energy to 14 ± 2 kJ mol^{-1} and the barrier to 135 ± 5 kJ mol^{-1} at a cluster size of 5 Å, which contains 11 tetrahedral (Si or Al) atoms. We embedded quantum clusters of various sizes in larger clusters with total radii in the range 7−20 Å, using the universal force field as the lower level of theory in ONIOM. We found convergence to the same values as the constrained clusters, without the use of reactive force fields or periodic boundary conditions in the embedding procedure. For the reaction energy, embedded cluster calculations required smaller clusters than in vacuo calculations, reaching converged reaction energies for quantum systems containing at least 8 tetrahedral atoms. In addition, optimizations on embedded clusters required many fewer cycles, and hence much less CPU time, than did optimizations on comparable constrained clusters.

I. Introduction

Zeolites offer a versatile class of shape-selective catalysts for important chemical processes such as petroleum cracking and reforming.[1,2] Many catalytic processes in zeolites are activated by proton transfer from Brønsted acid sites: Si−OH−Al. Progress in steering such reactions would be fueled by enhanced understanding of the mechanisms that control proton transfer in zeolites, which can be provided by molecular modeling.[3,4] Studying proton transfer in bare zeolites is important for several reasons: (i) trends in catalytic activity have been correlated with proton-transfer rates,[5,6] (ii) several intriguing discrepancies remain among experimental probes of proton transfer in bare zeolites,[7−10] and (iii) computational methods needed to model complex reactions in zeolites can be validated on this relatively simpler process.[11−14] An important issue in modeling zeolite electronic structures is how to represent the extended nature of zeolites with tractable calculations. In this article, we benchmark two approaches for computing the reaction energy and barrier for the O(1) to O(4) proton transfer in H−Y zeolite.

Quantum calculations on small clusters have long been the staple for modeling zeolite electronic structures.[3,4] However, even when clusters are constrained to mimic the target zeolite, qualitative errors can arise.[15−23] We found this in our study of the O(1) to O(4) jump in H−Y modeled with

* Corresponding author e-mail: auerbach@chem.umass.edu.
[†] Department of Chemistry, University of Massachusetts.
[‡] Department of Chemical Engineering, University of Massachusetts.
[§] Gaussian, Inc.

10.1021/ct0501203 CCC: $30.25
Published on Web 08/20/2005

a "3T" cluster [≡Si−O(1)−Al(OH)$_2$−O(4)−Si≡].[24−26] Although protons are observed by neutron diffraction at O(1) but not at O(4),[27] our O(1) to O(4) reaction energies were found to be negligible, signaling a qualitative failing of the small cluster model. In addition to ignoring long-range forces and some hydrogen bonding, small clusters lack the steric constraints that characterize adsorption in zeolites, because the cluster may not represent enough of the zeolite cavity.

Several remedies can be considered for solving the problems of small cluster models. The simplest is to use progressively larger clusters in vacuo until desired properties converge.[21,28] It is clear that with increasing cluster size, more of the important local electronic and steric effects are included, while the effect of the terminating region diminishes when it is further separated from the proton transfer site. In that approach, one has the choice of fully relaxing the clusters or imposing some geometrical constraints based on structural data.

Two promising avenues for including long-range forces are periodic quantum calculations[29−31] and embedded clusters.[32−34] The periodic approach, which is typically based on density functional theory (DFT), is relatively straightforward and provides the only reliable method for testing approximations other than those in DFT itself.[35−37] However, in the present context periodic DFT calculations suffer from two main drawbacks: they are expensive, treating all atoms equally, even distant spectator atoms; and they can be applied only to zeolites with sufficiently small unit cells, wherein too many acid sites may be formed. These limitations steer us to the embedded cluster approach.

The embedded cluster idea generally involves breaking a total system (S) into an inner region (I) of chemical interest and an outer environment (O). For zeolites and other covalent-network solids, this partitioning inherently leaves dangling bonds, requiring special methods to saturate the bonding in I. In many implementations of embedding,[38] link atoms are added to the inner region, yielding a cluster (C). One then endeavors to simulate the cluster C with chemical accuracy (hi), while modeling region O with much cheaper methods (lo). The total potential energy is then approximated by

$$E_{\text{embed}} = E_{\text{lo}}(\text{S}) + [E_{\text{hi}}(\text{C}) - E_{\text{lo}}(\text{C})] \quad (1)$$

$$= E_{\text{hi}}(\text{C}) + [E_{\text{lo}}(\text{S}) - E_{\text{lo}}(\text{C})] \quad (2)$$

Although eqs 1 and 2 are identical, they offer different viewpoints on embedding. Equation 1 suggests a low-level treatment of the total system corrected by a high-level cluster calculation, while eq 2 implies a high-level cluster calculation corrected by a low-level treatment of the environment. Although the embedding approach is appealing, two main issues about embedding in zeolite science remain generally unknown: optimal low- and high-levels of theory and optimal sizes of cluster C and total system S. Below we take a systematic approach at addressing this latter issue; in a forthcoming publication, we will report on optimal low- and high-levels of theory for modeling proton transfer in zeolites.

Sauer and co-workers have published many seminal calculations of proton-transfer energies in bare zeolites.[39] Their recent work on embedding clusters with their QM-Pot code is based on the following approach:[12,13,39,40] (i) use periodic boundary conditions for the total system; (ii) use a well-tuned molecular mechanics potential for the low level of theory, preferably one that has been fitted to electronic structure data obtained at the same level used for quantum cluster calculations; (iii) use a shell-model potential for the low level, to account for some electronic polarization;[41,42] (iv) use a reactive potential function for the low level, to mimic energies associated with making and breaking bonds;[43,44] and (v) do not electronically polarize the quantum cluster by its environment, to avoid double counting such polarization which is already treated approximately at the low level. Using this approach, Sierka and Sauer calculated reaction energies and barriers for specific proton jumps in acidic chabazite, H−Y and H-ZSM-5.[13] For the O(1) to O(4) jump in H−Y zeolite, they obtained reaction energies in the range 10−22 kJ mol^{-1} and a bare barrier of 95−100 kJ mol^{-1}, and found that proton transfer barriers are generally increased by long-range forces.[12,13]

We have initiated a research program modeling reactions catalyzed by zeolites of various chemical compositions.[35] Our present study of proton transfer in bare zeolites represents a base case for calibrating methods for future study. To promote the widest applicability by zeolite modelers, we seek to benchmark embedding methods suitable for use with all elements without further parametrization. This represents a departure from the philosophy behind methods such as QM-Pot, which employ reactive force fields finely tuned for specific systems. This paper is our first in a series using the ONIOM embedding procedure[38] in the Gaussian quantum chemistry code.[45,46] We believe this to be a versatile combination for modeling zeolites[47−49] because the implementation of ONIOM in Gaussian allows partitioning into more than two layers and provides molecular mechanics, semiempirical and ab initio methods for each level of theory. In the present article, we show that reliable energies of proton transfer in zeolites can be obtained using smaller clusters embedded in larger clusters and using the universal force field (UFF),[50] a generic nonreactive force field, as the low level of theory. This represents progress toward a simpler prescription for using embedding methods to model zeolite-guest systems of arbitrary composition.

We compare results from constrained and embedded quantum clusters of the same size. In constrained clusters, terminal atoms are fixed at positions suggested by diffraction experiments, while embedded clusters are connected to larger networks. We refer to these as 'hard' and 'soft' restraints, respectively. By comparing clusters of the same size with hard and soft restraints, we determine how various methods of terminating a quantum cluster influence proton-transfer properties. One might imagine that imposing hard restraints would perturb structural and vibrational properties of proton transfer. To address this issue, we compute proton-transfer attempt frequencies and O−Al−O angles in most systems studied.

In the present study we do not include electrostatic interactions between the quantum region and its environment. In a forthcoming publication we will include these electro-

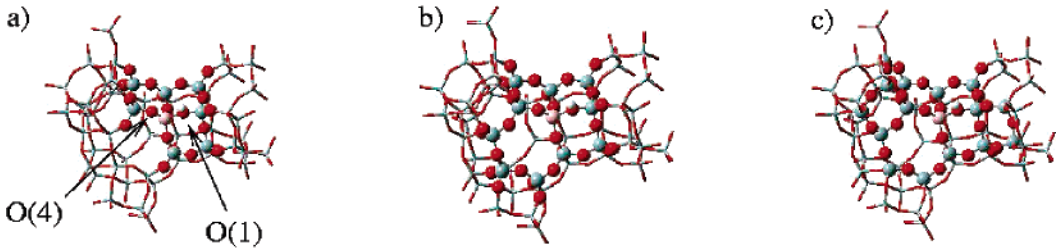

Figure 1. (a) 8T cluster embedded in a 53T system, also denoted 8T-16.95 Å, where 16.95 Å is the radius of the smallest sphere containing the entire system, with oxygens O(1) and O(4) labeled. (b) 11T cluster embedded in a 53T system (11T-16.95 Å). (c) 16T cluster embedded in a 53T system (16T-16.95 Å).

statics, incorporating charges from region O in the Hamiltonian of the quantum cluster.[51] Studying embedded clusters in this stepwise fashion allows us to disentangle mechanical and electronic embedding effects, thereby shedding further light on the energetics of reactions in zeolites.

The remainder of this article is organized as follows: in section II, we describe the zeolite clusters, electronic structure methods, and types of calculations performed. Section III details the results and discusses their implications, and in section IV we give concluding remarks.

II. Computational Methods

In this section, we describe the methods used to study the O(1) to O(4) proton jump in H−Y zeolite. First, we detail the zeolite clusters investigated and the methods used to incorporate properties of an extended system. We then review the electronic structure methods and geometry optimization techniques employed to compute energies, structures, and vibrational frequencies.

A. Zeolite Cluster Models. The chemical system under investigation is H−Y zeolite in the low-Al limit, where a single Si atom in the entire framework is replaced with an Al and charge balanced with a proton. The reaction in question is an internal proton transfer between crystallographically distinct oxygen atoms, O(1) and O(4). All of our models therefore feature a single Al tetrahedral site surrounded by a siliceous framework of varying size.

We study this internal proton transfer in quantum mechanically modeled clusters ranging in size from 3 tetrahedral centers (3T = Al + 2Si) to 22 tetrahedral centers (22T = Al + 21Si). We construct each cluster by clipping pieces from a crystal structure[27] of H−Y zeolite and terminating with hydrogen atoms at appropriate distances from atoms with dangling bonds. In constrained clusters, terminal hydrogens are placed along the vector toward the next atom in the zeolite framework at distances of 0.9 and 1.4 Å for Si−H and SiO−H termination, respectively. If a cluster is terminated primarily with Si−H bonds, the cluster is denoted as a "T-H" cluster; the O−H cluster termination is marked with "T-OH." Atoms were included in a cluster based on their distance from the Al. When necessary, atoms were added to complete a zeolite ring, which avoids placing terminal atoms in too close proximity when terminating dangling bonds. Figure 1 shows examples of various cluster sizes.

Terminating a molecular cluster fails to include the effects of excluded atoms; we attempt to include the most important of these effects through the use of geometric constraints placed on the cluster exterior. As outlined in the Introduction, we compare the effect of hard and soft restraints to gauge their influence on reaction energies. (We do not include fully relaxed clusters in our study, because they relax to rather nonzeolitic structures, especially for small clusters.) In cluster calculations with hard restraints (hereafter denoted "constrained"), the terminal hydrogen atoms are frozen in place, while all other atoms are allowed to relax. As in our previous work,[24] this serves to mimic the covalent "footprint" of the extended zeolite from which the cluster was clipped. Soft restraints are enforced by embedding a smaller cluster in a larger one (hereafter denoted "embedded"), using the Own N-Layer Integrated Molecular Orbital − Molecular Mechanics (ONIOM) method in GAUSSIAN quantum chemistry codes.[45,46] The embedded clusters differ from those in the constrained cluster calculations in the placement of the terminal hydrogens. In the case of constrained clusters, the terminal hydrogens are fixed in place through the entire optimization procedure, at positions determined from the crystal structure. In the case of embedded clusters, terminal hydrogens, also referred to as link atoms, are placed along the bond vectors pointing from the last shell of atoms in the cluster to the first shell of atoms in the outer ONIOM layer. Link atom positions vary during optimization because the outer ONIOM layer is itself flexible, except for terminal atoms on the boundary of the total system, whose positions are fixed at crystallographic locations.

B. Electronic Structure Methods. In an earlier study, we reported that constrained cluster models treated at the B3LYP/6-311G(d,p) level of theory yield accurate results for geometrical parameters and vibrational frequencies.[24] We also found that convergence of electronic energies is best obtained through the focal point method by correcting MP2/6-311G(d,p) energies with the difference {E[MP4/6-31G(d)] − E[MP2/6-31G(d)]}. In that same publication, we found that B3LYP/6-311G(d,p) underestimates reaction barriers by about 10 kJ mol^{-1} for this zeolite system, which is about 10% of the classical barrier height. This accuracy is deemed acceptable for the purposes of this study because such calculations provide a very good compromise between computational efficiency and accuracy. We thus employed the B3LYP/6-311G(d,p) level of theory as our high level throughout this work. Our ONIOM calculations use this basis set and level of theory to compute E_{hi}(C), while the Universal Force Field[50] (UFF) level of theory is used to compute E_{lo}(S) and E_{lo}(C) in eqs 1 and 2.

The choice of UFF for the low level of theory in our ONIOM calculations is justified in several ways. First, UFF contains parameters for all elements in the periodic table and as such provides a broadly applicable low level of theory. Though we do not exploit this generality in the present study, it may prove useful in future work. Second, using UFF allows us to test whether a nonreactive force field can produce accurate proton-transfer energies within ONIOM. The form of the ONIOM energy in eq 2 suggests this is possible, because unphysical energy terms that are introduced by bond breaking events identically cancel in the correction term $[E_{lo}(S) - E_{lo}(C)]$. Third, UFF as parametrized for silicates lacks partial charges. As such, this low level of theory is essentially a ball-and-spring model with minimal electronic effects, making it ideal for determining the influence of only network constraints, without additional complexities associated with long-range forces. This is consistent with our overall stepwise investigation into the various effects of the environment on proton transfer.

C. Calculation Details. We investigated convergence of four reaction parameters with respect to cluster sizes. These parameters are the reaction energy, activation energy, optimized O(1)−Al−O(4) angles for protons at O(1) and at O(4), and the vibrational frequency most closely associated with the O(1) to O(4) proton-transfer reaction coordinate. To compute these parameters, geometry optimizations of each cluster model were performed, followed by a vibrational frequency analysis.

The reaction energy and activation energy were computed as $\Delta E_{rxn} = E_{HO(4)} - E_{HO(1)}$ and $\Delta E_{act} = E_{TS} - E_{HO(1)}$, respectively. The reported energies do not include zero-point or thermal corrections. From these calculations, the O(1)−Al−O(4) angles at the reactant and product geometries were also recorded. In each individual geometry optimization, the cluster energy was converged to 10^{-6} Hartrees and the RMS force to 10^{-4} Hartrees a_o^{-1}. All transition states were confirmed to be first-order saddle points by computing and diagonalizing the mass-weighted Hessian matrix. We calculated vibrational frequencies with the masses of terminal atoms set to 10^6 au to mimic the macroscopic mass of the zeolite framework. For a subset of optimized constrained and embedded clusters, we report vibrational frequencies associated with the early stages of proton transfer, i.e., proton transfer "attempt frequencies".

Most embedding or QM/MM packages use a two-step or double-iteration method for geometry optimization.[34,52] In the first step, a geometry displacement is made only in the QM region (region I), while the MM region (region O) is kept frozen. For this step all the usual "small molecule" geometry optimization techniques are employed, such as a second-order approximation of the potential surface, Hessian update mechanisms, and the use of redundant internal coordinates. We note that QM/MM forces are used to determine the QM step, not just the QM forces. In the second step, the MM region is fully optimized, while the QM region is kept frozen. For this step we use a conjugate gradient optimizer in Cartesian coordinates, which is suitable for large systems. The two steps are repeated until convergence is reached.

The main reason for using this double-iteration method is that it remains intractable to use a second-order optimizer in redundant internal coordinates for very large systems. The required inversion or diagonalization of the Hessian is a computational bottleneck for larger systems, and the coordinate transformations become prohibitively expensive. With the double-iteration method, however, we still use a very accurate optimization method for the QM region, keeping the number of (expensive) QM energy and gradient evaluations to a minimum. The number of MM energy and gradient evaluations will increase significantly, but since these are several orders of magnitude cheaper than QM calculations, they have little effect on the total computational time.

The method outlined above, which uses relatively few "macroiterations" for the QM region and several more "microiterations" for the MM region, has been implemented in several QM/MM packages and has been used in numerous QM/MM studies. There are, however, several serious drawbacks of this scheme, related to the fact that the Hessian is only updated for the QM region. First, large displacements in the MM region, especially when a different local minimum is found, can lead to numerical instability of the Hessian update. Second, in the QM step, there is no direct coupling with the MM region, which deteriorates the quality of the QM step and increases the number of steps needed to reach convergence. Recently, we have addressed these issues by developing techniques that explicitly include coupling between the two regions in the QM step, while still using the double-iteration scheme.[53] This has significantly improved convergence behavior; indeed, we find no significant difference in performance between regular QM geometry optimization and QM/MM geometry optimizations. All the calculations were performed with GAUSSIAN03[45] and Gaussian Development Version[46] on Intel Linux workstations.

III. Results and Discussion

In this section, we describe the optimized geometries, reaction and activation energies, and vibrational frequencies obtained by the computational methods described above for modeling proton transfer from O(1) to O(4) in H−Y zeolite. We note that both experimental data and previous calculations agree that the reaction energy for this transfer should be endothermic, by 10−22 kJ mol^{-1} according to Sauer et al.,[12] which provides a broad target for our convergence studies.

A. Geometric Parameters. The O(1)−Al−O(4) angle affects proton-transfer kinetics by determining the jump distance and hence the activation energy of the reaction. Tables 1 and 2 show the values of O(1)−Al−O(4) angles from the constrained and embedded clusters for a variety of sizes. In Table 1, the O(1) results show reasonable convergence, and only the smallest (5T-H and 8T-H) constrained clusters are slightly off. In contrast, the angles of the embedded clusters (Table 2) are constant throughout the series, including the smallest clusters.

B. Reaction Energies. Table 3 summarizes our results for the proton-transfer reaction energy for both the con-

Table 1. OAlO Angle at Optimized Geometry from Constrained Cluster

	H on O(1)	H on O(4)
5T-H	93	93
8T-H	85	86
8T-OH	105	98
11T-OH	98	96
16T-OH	99	100
22T-OH	102	103

Table 2. OAlO Angle at Optimized Geometry from Embedded Cluster

	H on O(1)	H on O(4)
5T(H)-53T	99	99
8T(OH)-53T	101	105
16T(OH)-53T	100	98
16T(OH)-259T	100	97
22T(OH)-259T	101	100

strained and embedded clusters. Reaction energies of constrained zeolite clusters show stable convergence, reaching a value of 14 ± 2 kJ mol^{-1} at the 11T cluster size. The anomalously large reaction energy found for both 8T-H and 8T-OH clusters is due to a significant distortion of the reactant optimized structure allowed by floppiness of dihedral angles in terminal OSiOH groups. This effect is lessened both in larger clusters and in the ONIOM calculations. All constrained calculations correctly show that the transfer is endothermic. Extending the constrained cluster to include 22T atoms does not significantly affect ΔE_{rxn}, suggesting that convergence with respect to cluster size is reached. This suggestion is further corroborated by the ONIOM results below.

Using the ONIOM method, we seek convergence with respect to both the quantum cluster size and the total system size, which are represented as the rows and columns of Table 3, respectively. By scanning across any row, it is clear that changing the total system size has little effect on the reaction energy. At first this may be surprising, because the larger calculations include an order of magnitude more atoms. However, because the lower level of theory employed is UFF and therefore lacks long range forces in our calculations, there is only a local mechanical coupling between the inner and outer layers of the ONIOM model.

The size of the inner layer does, however, strongly affect the calculated reaction energy in approximately the same fashion as seen in the constrained cluster calculations. Here, the values for each total system size approach convergence at the 8T-OH quantum cluster size. Again, we observe that describing larger sections of the total system with a quantum mechanical method does not markedly improve the final result.

In our work all the larger clusters are terminated with hydroxyl groups; only for 8T can we compare the effect of hydrogen termination vs hydroxyl termination. We see indeed a large difference in the embedded 8T data, which was also reported by Brand et al. for proton affinities of acid sites in ZSM-5.[54]

In general, we find that a finite cluster, whether constrained or embedded, appears to be sufficient for predicting proton transfer reaction energies in zeolites. The use of methods based on periodic boundary conditions actually masks the length scales beyond which interactions no longer influence proton transfer. Determining such length scales is of fundamental importance for understanding how much of the zeolite actually controls reaction dynamics. The concept of a finite interaction length may come as a surprise considering that many researchers employ Ewald sums when simulating Coulombic interactions in partially ionic media such as zeolites.[55] Such long-range summations are crucial for calculating *absolute* adsorption energies of molecules in zeolites relative to vacuum. However, for calculating energy differences between nearby configurations of an adsorbed species, for example a reaction energy or barrier, the present results suggest that long-range interactions essentially cancel, leaving an energy difference controlled by local electronic interactions.

Our data suggest that this proton-transfer reaction is sensitive to atoms within ca. 5 Å of the reaction center. The presence of guest molecules will likely change this cutoff distance, but even in this more complex scenario we still expect a finite cluster to capture the reaction energetics. It is reasonable to surmise that using a low level of theory that includes electronic interactions would enable the use of even smaller inner regions in embedded calculations. We explore this possibility in future work.

C. Activation Energies. We calculated activation energies for constrained clusters and a subset of embedded clusters (Table 4). As discussed above, all transition states were confirmed to be first-order saddle points by the usual Hessian analysis. For the embedded clusters we considered total sizes of 53T and 166T. Although the number of data points is

Table 3. ΔE_{rxn} for O(1) to O(4) Proton Transfer[a]

		embedded (with size of full system in parentheses)					
cluster size	constrained	23 T (7 Å)	53 T (10 Å)	98 T (12.44 Å)	166T (14.8 Å)	259T (16.95 Å)	439T (19.91 Å)
3T−H	2.5	1.3	1.3	2.0	1.8	1.8	1.6
5T−H	4.3	5.4	5.9	6.9	6.5	6.4	6.3
8T−H	22.6	8.4	9.9	10.7	10.3	10.7	10.6
8T-OH	26.7		14.7	15.4	15.4	15.2	
11T-OH	13.6		14.4	14.9	15.0	14.8	
16T-OH	14.6					18.3	
22T-OH	13.8					15.4	

[a] In kJ mol^{-1}.

Table 4. ΔE_{act} for O(1) to O(4) Proton Transfer[a]

		embedded (with total size)	
cluster size	constrained	53T (10 Å)	166T (14.8 Å)
3T−H	90.2		118.9
5T−H	93.6	128.3	126.8
8T−H	57.3		134.7
8T-OH	138.8	137.8	139.2
11T-OH	133.4	133.7	136.5
16T-OH	131.6		132.7
22T-OH	138.8		

[a] In kJ mol^{-1}.

smaller than for the reaction energy, this still allows us to investigate convergence for both the total and quantum cluster size. From Table 4 we see that for embedded clusters, independent of total cluster size, the barrier converges at quantum cluster size 8T-OH. This was also the case for the reaction energy treated by embedded clusters (Table 3). The constrained barrier calculations also converge at quantum cluster size 8T-OH. These results further suggest that finite clusters, either constrained or embedded, can produce stable energetics of proton transfer in zeolites.

Our converged barrier is about 135 kJ mol^{-1} for both embedded and constrained clusters. For comparison, Sierka and Sauer obtained a barrier of about 100 kJ mol^{-1} for the same proton jump.[13] About 10 kJ mol^{-1} of this difference is a basis set effect. This was determined by repeating our computation of the barrier height in the 8T(OH)-53T embedded cluster using the Alrichs basis set used by Sierka and Sauer. This gave a barrier of 127.0 kJ mol^{-1}, as compared to 137.8 kJ mol^{-1} obtained using the 6-311G(d,p) basis set (see Table 4).

The remaining difference in barriers is harder to pin down. Our calculations and those of Sierka and Sauer differ mainly in the way volume is constrained and in the treatment of outer layer atoms. Regarding the former, we have built embedded and constrained zeolite clusters from diffraction data, fixing terminal atoms at experimentally determined locations. In contrast, Sierka and Sauer apply periodic boundary conditions at constant volume, with the lattice parameter determined from an initial force field optimization of the H−Y system at constant pressure. It is possible that our method of fixing terminal atoms can impose strain on reactant and transition state configurations. Such strain is expected to diminish as the total system size increases, thus placing terminal atom constraints farther away from the reaction center. However, the fact that barriers from our 8T-OH and 11T-OH quantum clusters (constrained and embedded) remain stable with respect to total system size suggests that our method of constraining volume does *not* impose unphysical strain on this proton-transfer process.

Our calculations and those of Sauer and Sierka also differ in the treatment of outer layer atoms. Our calculations represent electronic effects only in the quantum cluster, while those of Sierka and Sauer include classical electrostatics in the outer layer as well. It is possible that our local treatment of electronic effects can introduce errors into reactant and transition state energies. Such errors are expected to diminish as the quantum cluster size increases. The fact that barriers from quantum clusters 8T-OH and larger (constrained and embedded in Table 4) remain stable with respect to quantum cluster size suggests that our calculations include the electronic effects relevant for this proton transfer process. To pursue this point further, we will report in a forthcoming publication the results of fully periodic quantum calculations on this system.[15]

Table 5. Vibrational Frequency in Wavenumbers (cm^{-1}) for Constrained Cluster

	H on O(1)
5T−H	1054
8T-OH	1039
11T-OH	1011

Table 6. Vibrational Frequency in Wavenumbers (cm^{-1}) for Embedded Cluster

	H on O(1)	H on O(4)
5T(H)-23T	1064	1041
8T(H)-53T	1037	1030

Table 7. Calculation Times for Optimizing the System with the Proton at O(1)

system	av time per optimization cycle (h)	no. of optimization cycles	total CPU time (h)
22T-OH *constrained*	10.5	60	630
22T(OH)-259T *embedded*	10.7	20	213
11T-OH *constrained*	4.5	35	155
11T(OH)-259T *embedded*	4.9	20	98.8
8T-OH *constrained*	2.5	60	153
8T(OH)-53T *embedded*	2.6	20	51.8

D. Vibrational Frequencies. Vibrational frequencies are important dynamical parameters for quantifying activation entropies and attempt frequencies. Vibrational frequency analyses were performed on selected constrained and embedded clusters to test the convergence behavior of frequencies with respect to cluster size. Tables 5 and 6 show the vibrational frequency of the normal mode with the largest component of Al−O−H wag for the proton situated at O(1), which corresponds closely with the proton-transfer reaction coordinate.

Both sets of calculations show very similar vibrational frequencies for the H wag. The variation from one cluster size to another is smaller than the expected uncertainty of the electronic structure method. This is a bit surprising, considering that the hard termination inherent in constrained clusters might be expected to shift these to higher frequencies. However, our results suggest that either method of applying geometric constraints to the clusters is sufficient to achieve convergence of this particular dynamical parameter.

E. Computational Time Comparisons. In Table 7, we show CPU time comparisons for pairs of constrained and embedded calculations that contain identical quantum clusters. The times presented are for geometry optimizations starting from the crystal structure, with the acidic hydrogen added in a reasonable position relative to O(1). All timing

calculations were performed on dual processor 2.8 GHz PIV computers with 1 GB of core memory running Linux RedHat 9. Embedded cluster timings were obtained with the quadratically coupled QM/MM geometry optimization method.[45,46,53] For purposes of comparing CPU times, the optimizations were considered converged when the energy is stable to 0.00005 H (0.13 kJ mol^{-1}), which is the degree of precision we seek in our reaction energies. We allowed the optimizations to run significantly longer to test the robustness of this criterion and found only negligible changes in structure or energy. In Table 7, we also show the number of macroiterations required for geometry optimizations and the average CPU time required for each macroiteration.

In principle, we expect very similar times per optimization cycle for identical quantum clusters regardless of the method of constraint, because in the embedded calculations, the time used to compute energies and forces using UFF is negligible compared to the time spent in the quantum part of the calculation. This is precisely what we observe in Table 7. These timing data suggest that the principal difference between a constrained calculation and an embedded calculation on identical quantum clusters is simply the number of optimization cycles required to achieve convergence. In this respect, the constrained calculations appear to be *much slower* since they require many more optimization cycles. This poor convergence behavior may arise from a mismatch between floppy OSiOH dihedral angles and fixed terminal hydrogen atoms. More work is required to better understand this phenomenon.

Perhaps the most straightforward and important comparison in Table 7 is between the constrained and embedded cluster calculations that give converged reaction energies in the least time. These are the constrained 11T-OH and embedded 8T(OH)-53T systems, which converge in 155 and 51.8 CPU h, respectively. Thus, embedding speeds up these geometry optimizations by a factor of 3, despite the use of a generic low-level of theory (UFF) in ONIOM calculations.

IV. Concluding Remarks

We have studied the convergence properties of embedded and constrained cluster models of proton transfer in zeolites. We applied density functional theory to describe clusters and ONIOM to perform the embedding. We focused on converging the reaction energy and barrier of the O(1) to O(4) jump in H−Y zeolite as well as vibrational and structural aspects of this jump. We found that using successively larger clusters in vacuo gives convergence of the reaction energy to 14 ± 2 kJ mol^{-1}, and the barrier to 135 ± 5 kJ mol^{-1}, as long as the clusters are constrained to mimic zeolitic structures. These calculations converged for clusters with radii larger than 5 Å, containing at least 11 tetrahedral (Si or Al) atoms. We embedded quantum clusters of various sizes in larger clusters with total radii in the range 7−20 Å, using the universal force field (UFF) as the lower level of theory in ONIOM. We found convergence of the proton-transfer energy without the use of reactive force fields or periodic boundary conditions in the embedding procedure. Embedded cluster calculations gave converged reaction energies for quantum clusters containing at least 8 tetrahedral atoms. Optimizations on embedded clusters required many fewer cycles, and hence much less CPU time, than did optimizations on comparable constrained clusters.

Our present results suggest a reaction energy of 14 ± 2 kJ mol^{-1} and a barrier of 135 ± 5 kJ mol^{-1} for the O(1) to O(4) proton jump in H−Y zeolite. The smallest systems that yield reaction energies converged to within 1 kJ mol^{-1} of this value are the 11T-OH constrained cluster and the 8T(OH)-53T embedded cluster. These quantum clusters include atoms within ca. 5 Å of the reactive center. In future work, we will explore whether greater computational efficiency can be obtained by splitting the reactive region into two layers described by an accurate ab initio theory and a cheaper electronic theory, thereby giving a three-layer ONIOM calculation.[56] In the end, we aim for a simple and user-friendly method for modeling a wide variety of reactions in zeolites.

Acknowledgment. S.M.A. thanks the UMass Amherst Department of Chemistry for generous funding of our computer laboratory.

References

(1) *Handbook of Zeolite Science and Technology*; Auerbach, S. M., Carrado, K. A., Dutta, P. K., Eds.; Marcel Dekker: New York, 2003.

(2) Corma, A. *Chem. Rev.* **1995**, *95*, 559.

(3) Van Santen, R. A.; Kramer, G. J. *Chem. Rev.* **1995**, *95*, 637.

(4) Sauer, J. *Chem. Rev.* **1989**, *89*, 199.

(5) Farneth, W. E.; Gorte, R. J. *Chem. Rev.* **1995**, *95*, 615.

(6) Baba, T.; Ono, Y. *Appl. Catal. A* **1999**, *181*, 227.

(7) Baba, T.; Komastsu, N.; Ono, Y.; Sugaisawa, H. *J. Phys. Chem. B* **1998**, *120*, 804.

(8) Baba, T.; Komatsu, N.; Ono, Y.; Sugisawa, H.; Takahashi, T. *Microporous Mesoporous Mater.* **1998**, *22*, 203.

(9) Ernst, H.; Freude, D.; Mildner, T.; Pfeifer, H. High temperature ^{1}H MAS NMR studies of proton mobility in zeolites. In *Proceedings of the 12th International Zeolites Conference*; Treacy, M. M. J., Marcus, B. K., Bisher, M. E., Higghins, J. B., Eds.; MRS: Warrendale, PA, 1999; Vol. IV, p 2955.

(10) Sarv, P.; Tuherm, T.; Lippmaa, E.; Keskinen, K.; Root, A. *J. Phys. Chem.* **1995**, *99*, 13763.

(11) Brandle, M.; Sauer, J.; Dovesi, R.; Harrison, N. M. *J. Chem. Phys.* **1998**, *109*, 10379.

(12) Sauer, J.; Sierka, M.; Haase, F. Acid Catalysis by Zeolites: Ab Initio Modeling of Transition Structures. In *Transition State Modeling for Catalysis, Chapter 28*; Truhlar, D. G., Morokuma, K., Eds.; American Chemical Society: Washington, 1999; p 358.

(13) Sierka, M.; Sauer, J. *J. Phys. Chem. B* **2001**, *105*, 1603.

(14) Ryder, J. A.; Chakraborty, A. K.; Bell, A. T. *J. Phys. Chem. B* **2000**, *104*, 6998.

(15) Hill, J. R.; Freeman, C. R.; Delley, B. *J. Phys. Chem. A* **1999**, *103*, 3772.

(16) Limtrakul, J.; Khongpracha, P.; Jungsuttiwong, S.; Truong, T. N. *J. Mol. Catal. A* **2000**, *153*, 155.

(17) Limtrakul, J.; Nanok, T.; Jungsuttiwong, S.; Khongpracha, P.; Truong, T. N. *Chem. Phys. Lett.* **2001**, *349*, 161.

(18) Boronat, M.; Zicovich-Wilson, C. M.; Viruela, P.; Corma, A. *J. Phys. Chem. B* **2001**, *105*, 11169.

(19) Sinclair, P. E.; Vries, A. d.; Sherwood, P.; Catlow, C. R. A.; Van Santen, R. A. *J. Chem. Soc., Faraday Trans* **1998**, *94*, 3401.

(20) Rozanska, X.; Van Santen, R. A.; Hutschka, F.; Hafner, J. *J. Am. Chem. Soc.* **2001**, *123*, 7655.

(21) Zygmunt, S. A.; Curtiss, L. A.; Zapol, P.; Iton, L. E. *J. Phys. Chem. B* **2000**, *104*, 1944.

(22) Khaliullin, R. Z.; Bell, A. T.; Kazansky, V. B. *J. Phys. Chem. A* **2001**, *105*, 10454.

(23) Martinez-Magadan, J. M.; Cuan, A.; Castro, M. *Int. J. Quantum Chem.* **2002**, *88*, 750.

(24) Fermann, J. T.; Blanco, C.; Auerbach, S. M. *J. Chem. Phys.* **2000**, *112*, 6779.

(25) Fermann, J. T.; Auerbach, S. M. *J. Chem. Phys.* **2000**, *112*, 6787.

(26) Fermann, J. T.; Auerbach, S. M. *J. Phys. Chem. A* **2001**, *105*, 2879.

(27) Czjzek, M.; Jobic, H.; Fitch, A. N.; Vogt, T. *J. Phys. Chem.* **1992**, *96*, 1535.

(28) Gonzales, N. O.; Bell, A. T.; Chakraborty, A. K. *J. Phys. Chem. B* **1997**, *101*, 10058.

(29) Kresse, G.; Furthmuller, J. *Phys. Rev. B* **1996**, *54*, 11169.

(30) Civalleri, B.; D'Arco, P.; Orlando, R.; Saunders, V. R.; Dovesi, R. *Chem. Phys. Lett.* **2001**, *348*, 131.

(31) Shah, R.; Payne, M. C.; Lee, M. H.; Gale, J. D. *Science* **1996**, *271*, 1395.

(32) Sierka, M.; Sauer, J. *J. Comput. Chem.* **2000**, *21*, 1470.

(33) Greatbanks, S. P.; Sherwood, P.; Hillier, I. H. *J. Phys. Chem.* **1994**, *98*, 8134.

(34) Maseras, F.; Morokuma, K. *J. Comput. Chem.* **1995**, *16*, 1170.

(35) Astala, R.; Auerbach, S. M. *J. Am. Chem. Soc.* **2004**, *126*, 1843.

(36) Astala, R.; Auerbach, S. M.; Monson, P. A. *J. Phys. Chem. B* **2004**, *108*, 9208.

(37) Astala, R.; Auerbach, S. M.; Monson, P. A. *Phys. Rev. B* **2005**, *71*, 014112.

(38) Dapprich, S.; Komáromi, I.; Byun, K. S.; Morokuma, K.; Frisch, M. J. *J. Mol. Struct.-Theochem* **1999**, *461*−*462*, 1.

(39) Sauer, J.; Kolmel, C. M.; Hill, J.-R.; Ahlrichs, R. *Chem. Phys. Lett.* **1989**, *164*, 193.

(40) Sierka, M.; Sauer, J. *J. Chem. Phys.* **2000**, *112*, 6983.

(41) Catlow, C. R. A.; Dixon, M.; Mackrodt, W. C. In *Computer Simulations of Solids*; Catlow, C. R. A., Mackrodt, W. C., Eds.; Springer-Verlag: Berlin, 1982; Vol. 166, p 130.

(42) Gale, J. D. *J. Chem. Soc., Faraday Trans.* **1997**, *93*, 629.

(43) Aqvist, J.; Warshel, A. *Chem. Rev.* **1993**, *93*, 2523.

(44) Chang, Y.-T.; Miller, W. H. *J. Phys. Chem.* **1990**, *94*, 5884.

(45) Frisch, M. J.; Trucks, G. W.; Schlegel, H. B.; Scuseria, G. E.; Robb, M. A.; Cheeseman, J. R.; Montgomery, J. A., Jr.; Vreven, T.; Kudin, K. N.; Burant, J. C.; Millam, J. M.; Iyengar, S. S.; Tomasi, J.; Barone, V.; Mennucci, B.; Cossi, M.; Scalmani, G.; Rega, N.; Petersson, G. A.; Nakatsuji, H.; Hada, M.; Ehara, M.; Toyota, K.; Fukuda, R.; Hasegawa, J.; Ishida, M.; Nakajima, T.; Honda, Y.; Kitao, O.; Nakai, H.; Klene, M.; Li, X.; Knox, J. E.; Hratchian, H. P.; Cross, J. B.; Adamo, C.; Jaramillo, J.; Gomperts, R.; Stratmann, R. E.; Yazyev, O.; Austin, A. J.; Cammi, R.; Pomelli, C.; Ochterski, J. W.; Ayala, P. Y.; Morokuma, K.; Voth, G. A.; Salvador, P.; Dannenberg, J. J.; Zakrzewski, V. G.; Dapprich, S.; Daniels, A. D.; Strain, M. C.; Farkas, O.; Malick, D. K.; Rabuck, A. D.; Raghavachari, K.; Foresman, J. B.; Ortiz, J. V.; Cui, Q.; Baboul, A. G.; Clifford, S.; Cioslowski, J.; Stefanov, B. B.; Liu, G.; Liashenko, A.; Piskorz, P.; Komaromi, I.; Martin, R. L.; Fox, D. J.; Keith, T.; Al-Laham, M. A.; Peng, C. Y.; Nanayakkara, A.; Challacombe, M.; Gill, P. M. W.; Johnson, B.; Chen, W.; Wong, M. W.; Gonzalez, C.; Pople, J. A. Gaussian 03; Revision C.02 ed.; Gaussian, Inc.: Wallingford, CT, 2004.

(46) Frisch, M. J.; Trucks, G. W.; Schlegel, H. B.; Scuseria, G. E.; Robb, M. A.; Cheeseman, J. R.; Montgomery, J. A., Jr.; Vreven, T.; Kudin, K. N.; Burant, J. C.; Millam, J. M.; Iyengar, S. S.; Tomasi, J.; Barone, V.; Mennucci, B.; Cossi, M.; Scalmani, G.; Rega, N.; Petersson, G. A.; Nakatsuji, H.; Hada, M.; Ehara, M.; Toyota, K.; Fukuda, R.; Hasegawa, J.; Ishida, M.; Nakajima, T.; Honda, Y.; Kitao, O.; Nakai, H.; Klene, M.; Li, X.; Knox, J. E.; Hratchian, H. P.; Cross, J. B.; Adamo, C.; Jaramillo, J.; Gomperts, R.; Stratmann, R. E.; Yazyev, O.; Austin, A. J.; Cammi, R.; Pomelli, C.; Ochterski, J. W.; Ayala, P. Y.; Morokuma, K.; Voth, G. A.; Salvador, P.; Dannenberg, J. J.; Zakrzewski, V. G.; Dapprich, S.; Daniels, A. D.; Strain, M. C.; Farkas, O.; Malick, D. K.; Rabuck, A. D.; Raghavachari, K.; Foresman, J. B.; Ortiz, J. V.; Cui, Q.; Baboul, A. G.; Clifford, S.; Cioslowski, J.; Stefanov, B. B.; Liu, G.; Liashenko, A.; Piskorz, P.; Komaromi, I.; Martin, R. L.; Fox, D. J.; Keith, T.; Al-Laham, M. A.; Peng, C. Y.; Nanayakkara, A.; Challacombe, M.; Gill, P. M. W.; Johnson, B.; Chen, W.; Wong, M. W.; Gonzalez, C.; Pople, J. A. Gaussian Development Version; Revision C.01 ed.; Gaussian, Inc.: Wallingford, CT, 2004.

(47) Damin, A.; Bordiga, S.; Zecchina, A.; Lamberti, C. *J. Chem. Phys.* **2002**, *117*, 226.

(48) Damin, A.; Bonino, F.; Ricchiardi, G.; Bordiga, S.; Zecchina, A.; Lamberti, C. *J. Phys. Chem. B* **2002**, *106*, 7524.

(49) Sillar, K.; Purk, P. *J. Mol. Struct.-Theochem.* **2002**, *589*, 281.

(50) Rappe, A. K.; Casewit, C. J.; Colwell, K. S.; Goddard, W. A.; Skiff, W. M. *J. Am. Chem. Soc.* **1992**, *114*, 10024.

(51) Vreven, T.; Morokuma, K. *Theor. Chem. Acct.* **2003**, *109*, 125.

(52) Vreven, T.; Morokuma, K.; Farkas, Ö.; Schlegel, H. B.; Frisch, M. J. *J. Comput. Chem.* **2003**, *24*, 760.

(53) Vreven, T.; Frisch, M. J.; Kudin, K. N.; Schlegel, H. B.; Morokuma, K. *Mol. Phys.* **2005**, in press.

(54) Brand, H. V.; Curtiss, L. A.; Iton, L. E. *J. Phys. Chem.* **1992**, *96*, 7725.

(55) Auerbach, S. M.; Jousse, F.; Vercauteren, D. P. Dynamics of Sorbed Molecules in Zeolites. In *Computer Modelling of Microporous and Mesoporous Materials*; Catlow, C. R. A., Van Santen, R. A., Smit, B., Eds.; Academic Press: London, 2004; p 49.

(56) Vreven, T.; Morokuma, K. *J. Comput. Chem.* **2000**, *21*, 1419.

CT0501203